ACI STRUCTURAL JOURNAL TECHNICAL PAPER

Title no. 86-S27

Lateral Displacement Ductility of Reinforced Concrete Flat Plates

by Austin Pan and Jack P. Moehle

It is presently unclear whether the reinforced concrete flat-slab connection possesses sufficient lateral displacement capacity to survive the lateral deformations that can be expected during a strong earthquake. The objective of this paper is to examine the available data from present and past research and from there develop an understanding of the major parameters that influence the lateral displacement capacity and ductility of reinforced concrete flat plates. The significant effects of gravity load and biaxial lateral loading are presented together with the implications of the findings with regard to seismic design and performance. It is recommended that to insure adequate displacement ductility under extreme earthquake loading, the gravity level shear stress acting on the slab critical section be limited to $1.5\sqrt{f'_c}$ *psi.*

Keywords: biaxial loads; buildings; **ductility; earthquake-resistant structures; flat concrete plates; lateral pressure;** reinforced concrete; shear strength; structural design.

In design of buildings to resist earthquake ground motions, the prevailing ductile design philosophy typically requires that elements of the structural system be capable of deforming into the inelastic range. This requirement often, but not always, extends to elements that are not considered in design as part of the lateral load-resisting system. For example, a common form of construction in seismic zones in the United States combines flat-plate frames to carry gravity loads with shearwalls to resist the earthquake loads. It is unclear in this form of construction whether the flat-plate connection will possess sufficient lateral displacement capacity to survive the lateral deformations that can be reasonably expected during a strong earthquake.

The objective of this paper is to examine the available data, and from that develop an understanding of the major parameters that influence the lateral displacement capacity and ductility of reinforced concrete flat plates. The significant effects of gravity load and biaxial lateral loading are presented. Implications of the findings with regard to seismic design and performance are discussed.

REVIEW OF EXPERIMENTAL OBSERVATIONS

Experimental data from several research investigations reported in the literature were gathered for this study (Table 1). Included are data from Hawkins, Mitchell, and Sheu;[1] Morrison and Sozen;[2] Ghali, Elmasri, and Dilger;[3] Islam and Park;[4] Hanson and Hanson;[5] Zee and Moehle,[6] Symonds, Mitchell, and Hawkins;[7] and recent tests conducted by the authors (Appendix I). Prerequisites for selection of these data were that: (1) specimens represented interior connections, (2) specimens contained no slab shear reinforcement, and (3) specimens were loaded to simulate effects of shears and moments due to vertical and lateral loads. Some of the specimens (No. 1 through 11 and 15 through 21) were subjected to reversed cyclic lateral loads simulating severe seismic loading. Others (No. 12 through 14 and 22 through 23) were subjected to effectively monotonic lateral loading.

Relevant data of these experiments are tabulated in Table 1. Brief descriptions of the specimens, test procedures, and principal results follow. More detailed information can be found in the original papers.[1-7] Appendix I provides details of recent tests by the authors (on Specimen No. 16 through 19) that have not been reported previously in the literature.

Test descriptions

All of the test specimens reported herein were similar in that a single interior connection subassemblage was isolated from an idealized structure, and loads were applied to simulate lateral load effects (Fig. 1). The column in each test specimen extended above and below the slab to pinned connections located at a point equivalent to the column midheight of an idealized building. In the direction parallel to lateral loading, the

ACI Structural Journal, V. 86, No. 3, May-June 1989.
Received Oct. 27, 1987, and reviewed under Institute publication policies.

Austin Pan is an assistant professor at Purdue University, West Lafayette, Indiana. He received his BS from the University of Texas at Austin and his MS and PhD degrees in civil engineering from the University of California at Berkeley. Pan previously was a structural engineer with T. Y. Lin International, San Francisco.

ACI member Jack P. Moehle is an associate professor of civil engineering at the University of California at Berkeley. He received the BS, MS, and PhD (1980) degrees from the University of Illinois at Urbana-Champaign. He is a member of ACI-ASCE Committees 352, Joints and Connections, and 442, Response to Lateral Forces. He is active in research on behavior and design of flat-slab structures subjected to vertical and lateral loads.

slab extended on either side to a point equivalent to midspan of the prototype slab, except for Specimens 1 through 6, which extended 0.3 times the slab span. In the transverse direction, the total slab width ranged between half the longitudinal span and the full longitudinal span.

Slab gravity loads were simulated in some of the tests (Specimens 1 through 6, 10 through 11, and 15 through 21). The procedure of adding these vertical loads varied; in some cases subsidiary weights were placed on the slab surface (Specimens 10 through 11 and 15 through 21), and in other cases vertical actuators applied the load (Specimens 1 through 6).

In some of the tests (Specimens 7 through 19), lateral load effects were simulated by attaching the slab edge to roller supports and then loading laterally at the top of the column [Fig. 1(a)]. In the other tests, lateral load effects were simulated by actuators that applied equal and opposite vertical loads to the ends of the slab while the columns were restrained against lateral dis-

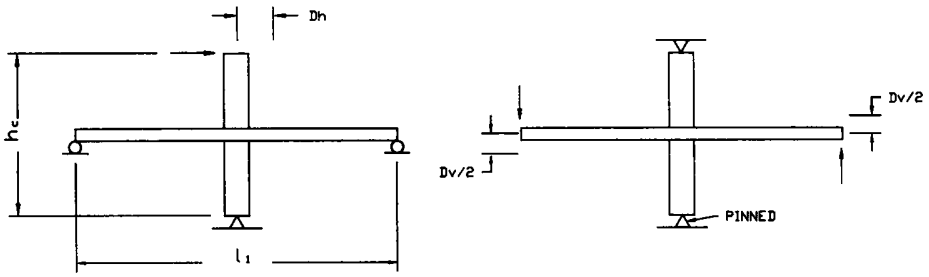

(a) Lateral Load at Column *(b) Vertical Load at Slab Ends*

Fig. 1—Lateral load simulation

Table 1 — Data of experimental specimens

Specimen number	Label*	Researchers	c_1, in.	c_2, in.	h, in.	d_{ave}, in.	l_1, in.	l_2, in.	h_c, in.	$p_{t,c+3h}$	$p_{b,c+3h}$	f_y, psi	f'_c, psi
1	S1	Hawkins et al.[1]	12.0	12.00	6.00	4.60	144	84	102	0.0120	0.00590	66,600	5050
2	S2		12.0	12.00	6.00	4.60	144	84	102	0.0084	0.00490	67,100	3400
3	S3		12.0	12.00	6.00	4.60	144	84	102	0.0055	0.00400	66,000	3200
4	S4		12.0	12.00	6.00	4.60	144	84	102	0.0120	0.00590	66,600	4690
5	S6	Symonds et al.[7]	12.0	12.00	6.00	4.60	144	84	102	0.0181	0.00910	66,600	3360
6	S7		12.0	12.00	6.00	4.60	144	84	102	0.0084	0.00490	67,100	3840
7	S1	Morrison and Sozen[2]	12.0	12.00	3.00	2.36	72	72	44	0.0065	0.00650	46,800	6640
8	S2		12.0	12.00	3.00	2.36	72	72	44	0.0098	0.00980	47,900	5090
9	S3		12.0	12.00	3.00	2.36	72	72	44	0.0131	0.01310	48,600	4920
10	S4		12.0	12.00	3.00	2.36	72	72	44	0.0098	0.00980	46,000	5060
11	S5		12.0	12.00	3.00	2.36	72	72	44	0.0098	0.00980	49,300	5110
12	SM 0.5	Ghali et al.[3]	12.0	12.00	6.00	4.75	72	72	46	0.0050	0.00167	69,000	5329
13	SM 1.0		12.0	12.00	6.00	4.75	72	72	46	0.0100	0.00333	69,000	4835
14	SM 1.5		12.0	12.00	6.00	4.75	72	72	46	0.0150	0.00500	69,000	5794
15	INT	Zee and Moehle[6]	5.4	5.40	2.40	1.99	72	72	36	0.0080	0.00600	63,100	5400
16	AP1	Authors	10.8	10.80	4.84	4.07	144	144	72	0.0086	0.00290	70,200	4250
17	AP2		10.8	10.80	4.84	4.07	144	144	72	0.0086	0.00290	70,200	4400
18	AP3		10.8	10.80	4.84	4.07	144	144	72	0.0086	0.00290	70,200	4600
19	AP4		10.8	10.80	4.84	4.07	144	144	72	0.0086	0.00290	70,200	4500
20	IP2	Islam and Park[4]	9.0	9.00	3.50	2.75	108	90	60	0.0106	0.00534	54,200	4630
21	IP3C		9.0	9.00	3.50	2.75	108	90	60	0.0106	0.00534	45,800	4310
22	B7	Hanson and Hanson[5]	12.0	6.00	3.00	2.25	72	48	63	0.0150	0.01500	51,400	4780
23	C8		6.0	12.00	3.00	2.25	72	48	63	0.0150	0.01500	59,600	4760

*Designation used by original researchers.
†Top steel ratio within $C_2 + 3h$ strip over column.
‡Bottom steel ratio within $C_2 + 3h$ strip over column.
1 in. = 25.4 mm; 1 psi = 6895 Pa.

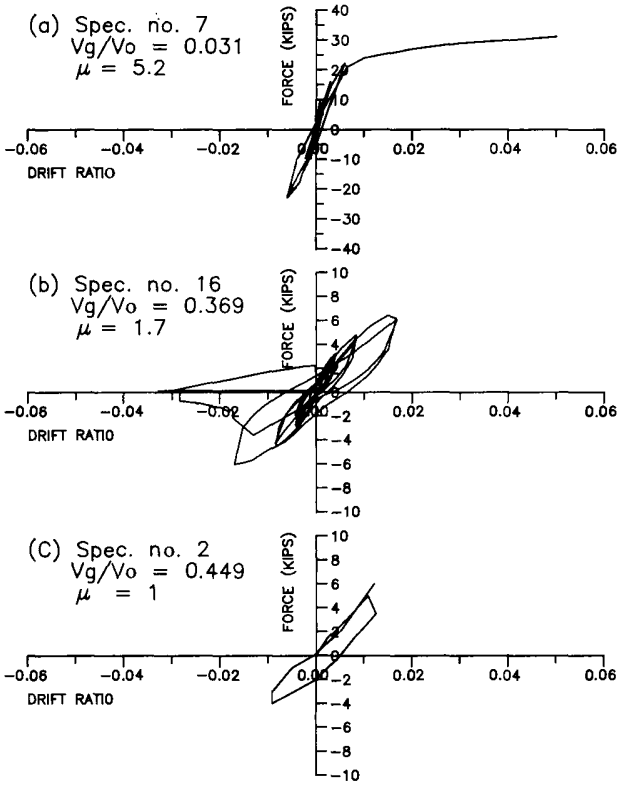

Fig. 2—Classification of specimen response (1 kip = 4.448 kN)

placement [Fig. 1(b)]. There is no general agreement as to which of these two testing techniques is more representative of actual conditions. Both probably represent situations to which a redundant, nonlinear building system is exposed.

All tests reported previously in the literature have considered only uniaxial lateral loadings. The tests by the authors (Specimens 16 through 19) considered both uniaxial and biaxial lateral loadings, as reported in Appendix I.

Lateral load-displacement relations

For those specimens that were tested by laterally displacing the upper column (Specimens 7 through 19), the lateral load-displacement relation is self-evident from measured lateral loads and displacements at the top of the upper column. For the specimens that were loaded by vertically displacing the slab ends (Specimens 1 through 6 and 20 through 23), the lateral load (reaction at the upper column) was resolved by statics. Lateral displacement of the specimen D_h was taken as

$$D_h = D_v(h_c/l_1) \quad (1)$$

in which D_v is the difference of the vertical displacements at opposite ends of the slab at the point of vertical load application; h_c is total column height; and l_1 is the length of span of the slab in the direction of lateral loading (see Fig. 1). For Specimens 1 through 6, effective lateral displacements D_h obtained by Eq. (1) were further multiplied by a factor 1/0.6 because, as described in References 1 and 7, the slab span of the specimens represents approximately 0.6 times the total span of the slab in the prototype.

Measured lateral load-displacement relations from three of the specimens that were subjected to reversed cyclic lateral loads are plotted in Fig. 2. These relations display the broad range of behaviors observed for the connections included in this study. The data in Fig. 2(a) reveal a relatively stable hysteretic response to lateral drifts well beyond the range of practical interest in building design.

The data in Fig. 2(b) also reveal a stable hysteretic response, but to significantly less drift than obtained for the specimen in Fig. 2(a). Failure occurred in a relatively sudden punching shear mode after the slab reinforcement near the column had yielded. Lateral drift at which failure occurred in this case can be reasonably expected for a multistory building subjected to an intense earthquake motion.[8] Unless measures are taken to control lateral drift, this connection may not be suitable in a building designed to resist strong earthquakes. Fig. 2(c) presents a response history that is even further curtailed by punching shear failure. The low level of lateral drift and complete lack of apparent ductility make this type of specimen clearly unsuitable for almost all types of buildings subject to severe earthquake loading.

It is useful to classify responses of the specimens in Table 1 qualitatively according to the response types depicted in Fig. 2. The assigned classifications—either A, B, or C, signifying behavior similar to that plotted in Fig. 2(a), (b), or (c), respectively, are indicated in Table 2.

Two measures are used in this study to quantify the lateral deformation capacities of the specimens. The first measure is the maximum drift, which is defined as the lateral drift at failure D_u as a percent of specimen height h_c. Lateral drift at failure is tabulated for each specimen in Table 2.

The second measure of deformation capacity is the lateral displacement ductility at failure μ. Lateral displacement ductility cannot be defined uniquely for slab-column connections because the force-displacement relation has no distinct yield point (because yield spreads gradually across the slab transverse width).

To overcome the uncertainty in defining the yield displacement, an arbitrary procedure was applied. The procedure, illustrated in Fig. 3, was first to construct the envelope relation between lateral displacement and lateral load. The envelope relation was then idealized by an elastoplastic relation. The initial slope of the idealized relation is a secant through the measured relation at a load equal to two-thirds of the measured strength. The plastic portion of the idealized relation passes through the maximum load and the maximum deformation at failure. The intersection between these two lines defines an effective yield displacement.

Displacement ductility is then calculated as the ratio between the ultimate displacement and yield displacement ($\mu = D_u/D_y$) of the idealized relation (Fig. 3). The computed lateral displacement ductilities μ for the test specimens are listed in Table 2.

Table 2 — Summary of analysis results

Specimen number	Label	Researchers	V_g, kips	Ductility ratio	Maximum drift, percent	V_g/V_o	Classification
1	S1	Hawkins et al.[1]	28.80	1.58	3.75	0.332	A
2	S2		32.00	1.00	2.00	0.449	C
3	S3		31.20	1.00	2.00	0.451	C
4	S4		33.70	1.90	2.60	0.403	B
5	S6	Symonds et al.[7]	61.00	1.00	1.10	0.861	C
6	S7		61.00	1.00	1.00	0.806	C
7	S1	Morrison and Sozen[2]	1.35	5.20	4.70	0.031	A
8	S2		1.35	2.90	2.80	0.035	B
9	S3		1.35	3.90	4.20	0.035	A
10	S4		3.00	4.20	4.50	0.078	A
11	S5		6.42	4.00	4.80	0.166	A
12	SM 0.5	Ghali et al.[3]	29.00	3.50	6.00	0.312	A
13	SM 1.0		29.00	1.40	2.70	0.328	B
14	SM 1.5		29.00	1.80	2.70	0.299	B
15	INT	Zee and Moehle[6]	3.60	3.20	3.30	0.208	B
16	AP1	Authors	23.32	1.70	1.60	0.369	B
17	AP2		23.32	1.87	1.50	0.363	B
18	AP3		12.00	2.32	3.70	0.183	B
19	AP4		12.00	2.11	3.50	0.185	B
20	IP2	Islam and Park[4]	6.42	3.20	5.00	0.182	A
21	IP3C		7.64	4.00	4.00	0.225	B
22	B7	Hanson and Hanson[5]	1.10	3.40	3.80	0.039	B
23	C8		1.26	2.80	5.80	0.045	A

1 kip = 4.448 kN.

EFFECT OF GRAVITY LOAD ON LATERAL DISPLACEMENT DUCTILITY

The level of gravity load carried by the slab is a primary variable affecting the apparent lateral ductility. This phenomenon has been identified in earlier tests by Kanoh and Yoshizaki.[9] The same trend is apparent in the relations plotted in Fig. 2. In that figure, lateral displacement ductility decreases from Fig. 2(a) to 2(c) as gravity load carried by the slab increases.

To generalize the conclusion that gravity load affects lateral displacement capacity of the connection, lateral displacement ductility μ (Table 2) was plotted versus the normalized gravity shear ratio V_g/V_o (Table 2) for each connection. The value V_g is the vertical shear acting at failure on the slab critical section defined at a distance $d/2$ from the column face in which d is the average slab effective depth. The quantity V_o is the theoretical punching shear strength in the absence of moment transfer, as given for these connections by Eq. (2)[11]

$$V_o = 4\sqrt{f'_c}\, b_o d \qquad (2)$$

in which V_o is in lb; f'_c equals the compressive strength of concrete in psi; and b_o equals the perimeter length of the slab critical section (b_o and d are given in in.).

The relation between lateral displacement ductility μ and the gravity shear ratio V_g/V_o is plotted in Fig. 4. Clearly, for values of V_g/V_o exceeding approximately 0.4, there is virtually no lateral displacement ductility (μ = 1.0); that is, the connection fails by punching before any yield in the load-displacement relation is detected. As gravity shear decreases, there is an increase in the available ductility.

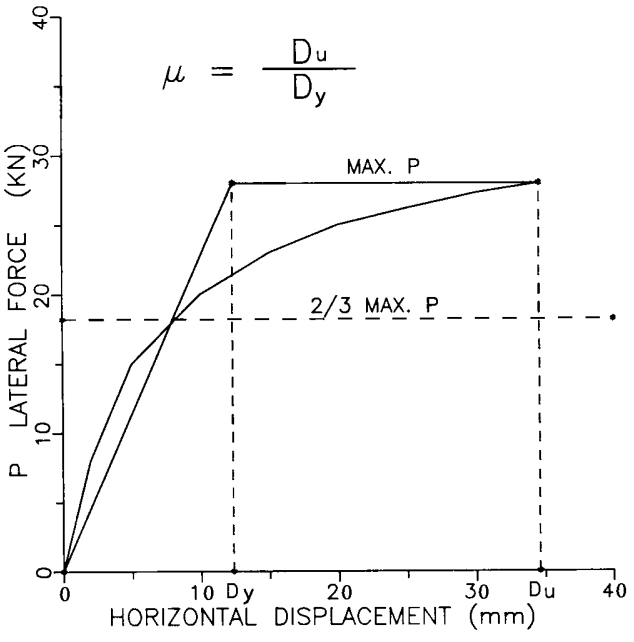

Fig. 3—Definition of displacement ductility (1 kN = 0.225 kip; 1 mm = 0.029 in.)

The effect of gravity shear on lateral drift at failure is presented in Fig. 5. As in Fig. 4, there is a reduction in available drift with increasing gravity shear ratio.

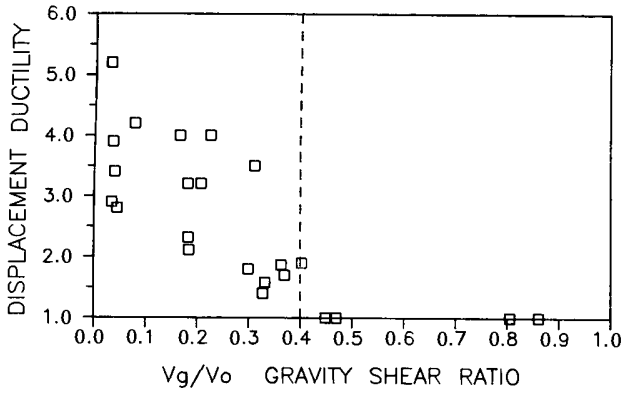

Fig. 4—Effect of gravity load on ductility

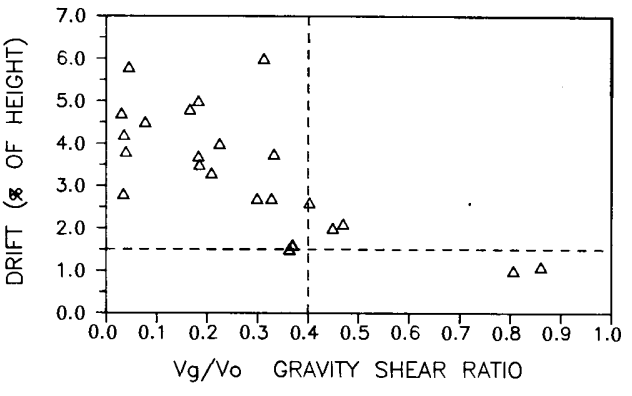

Fig. 5—Effect of gravity load on drift

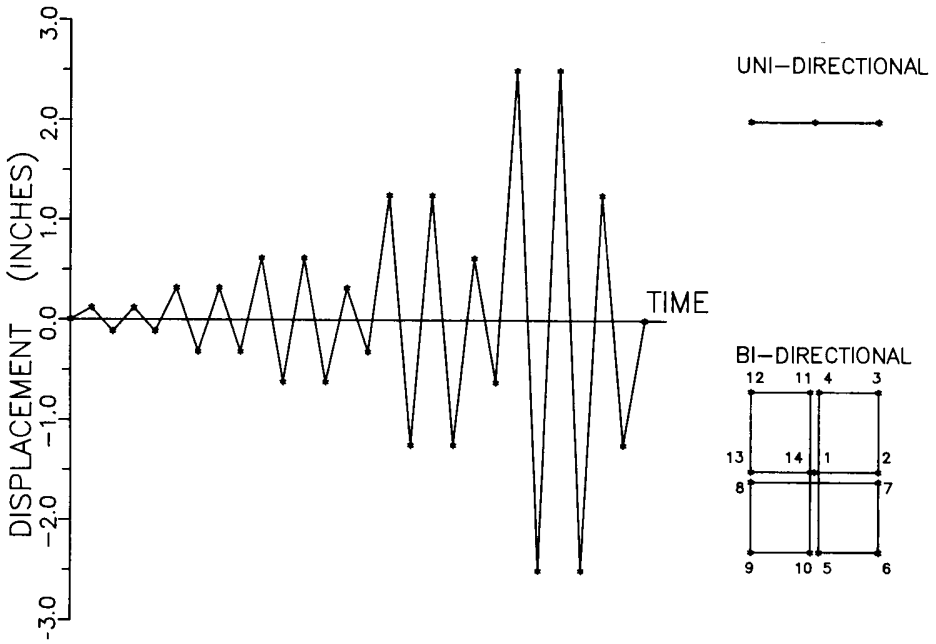

Fig. 6—Lateral displacement history and loading patterns (1 in. = 25.4 mm)

The observation that lateral deformation capacity and gravity shear are related is not surprising and has been identified previously.[1,4] According to the ACI Building Code,[11] shear strength for square interior columns is defined by Eq. (2). This limiting shear strength has been established from tests of slab-column connections for which shear failure occurred before widespread yielding of the slab reinforcement.[12]

The condition for which this limiting shear stress is defined is consistent with the philosophy of the main body of the ACI Building Code, namely, that design loads are set sufficiently high and inelastic redistribution is limited sufficiently that significant yield at connections will not occur. Under this loading condition, the surrounding slab confines the connection region. This confinement is believed to be the reason why observed nominal shear stresses at failure are larger for slab-column connections than for linear elements such as beams.[10]

Some researchers[12] have hypothesized that the confining effect of the slab is diminished when widespread yield of the slab reinforcement occurs in the connection region. Experimental data in support of this hypothesis have been presented previously for connections loaded solely by vertical loads.[12] The data for lateral load tests presented in Fig. 4 augment these vertical load data.

EFFECT OF BIAXIAL LATERAL LOADING ON LATERAL DISPLACEMENT DUCTILITY

During wind or earthquake loading, the slab-column connection resists lateral loads acting in multiple directions. To investigate the influence of biaxial lateral loading, four specimens were tested by the authors. Limited details of the tests are presented for reference in Appendix I. In the test program, two specimens were tested with a uniaxial lateral displacement history, one with high gravity load (AP1), and one with relatively low gravity load (AP3). Nominally identical specimens (AP2 and AP4) subsequently were subjected to biaxial lateral load histories. The displacement histories are compared in Fig. 6. The biaxial load history followed sequentially Points 1 through 14 as indicated in Fig. 6.

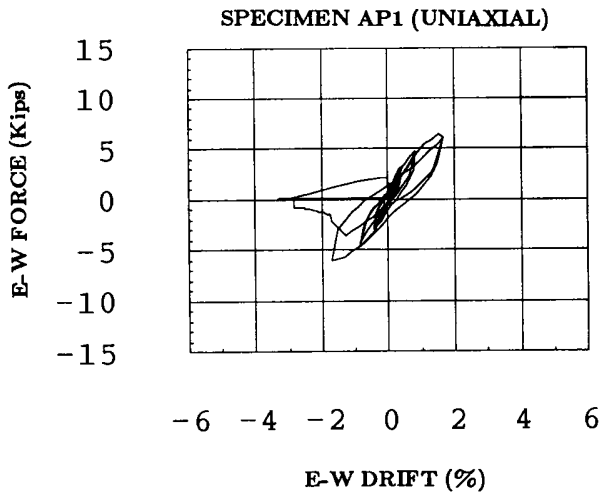

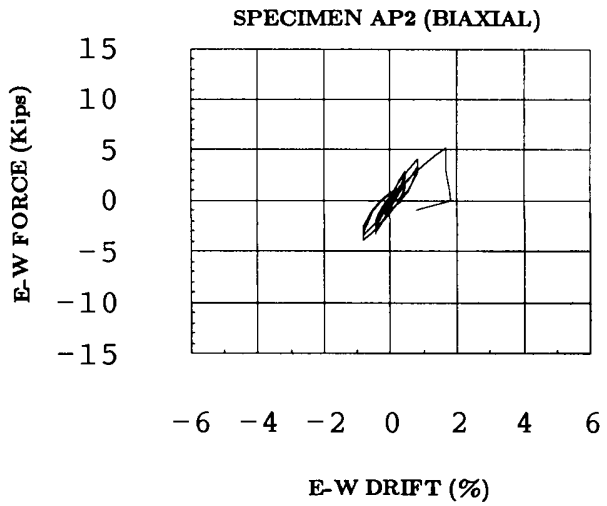

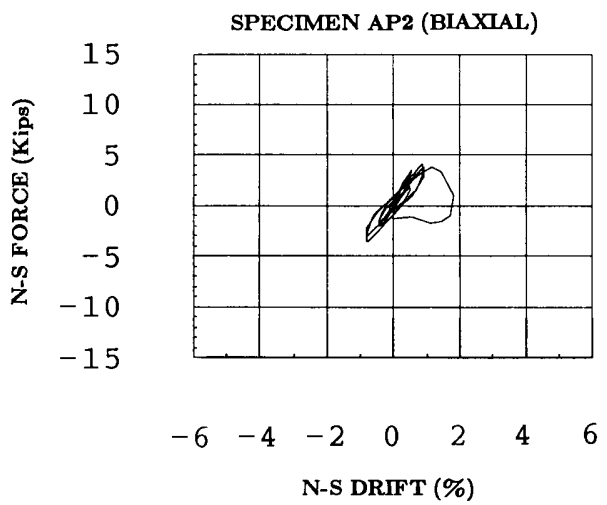

Fig. 7—Uniaxial and biaxial tests (high gravity load) (1 kip = 4.448 kN)

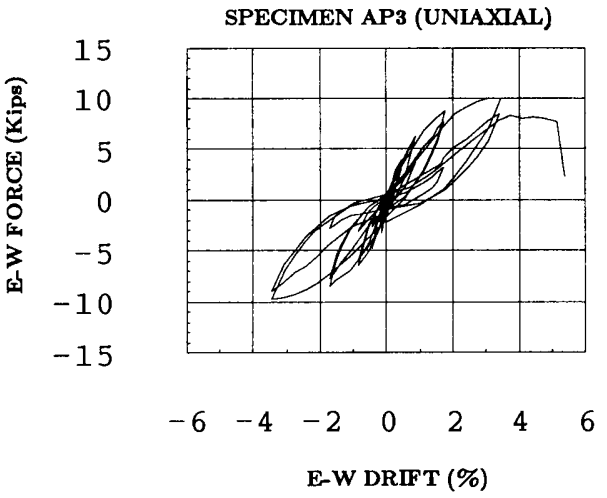

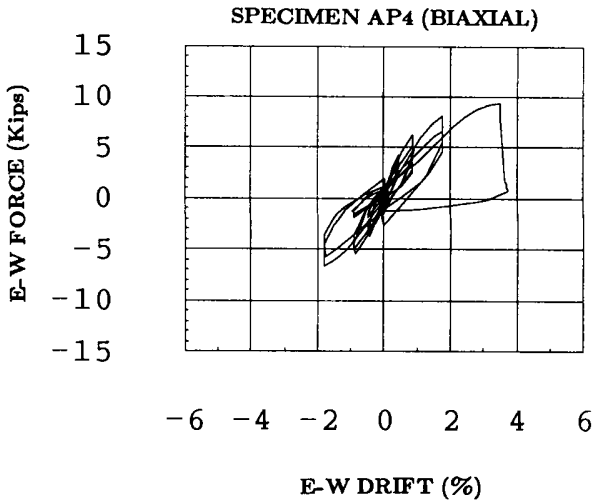

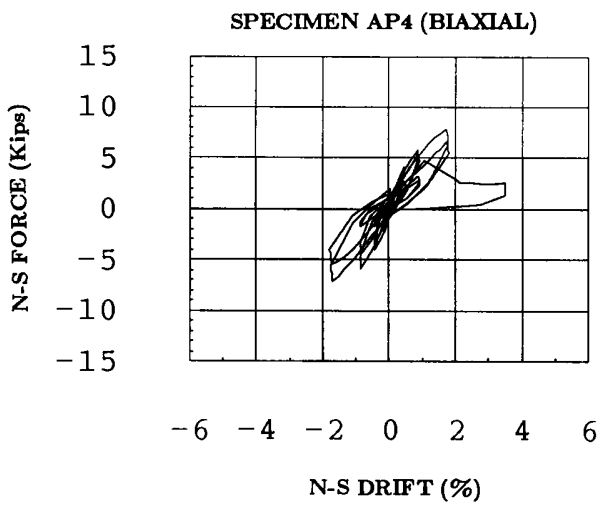

Fig. 8—Uniaxial and biaxial tests (low gravity load) (1 kip = 4.448 kN)

Fig. 7 and 8 show the measured relations between lateral force and lateral drift. As can be observed in those figures, the biaxially loaded specimens (AP2 and AP4) failed at an earlier stage of testing in comparison with the companion uniaxially loaded specimens. Both stiffness and strength were less for the biaxially loaded specimens than for the equivalent uniaxially loaded specimens.

The lower resistance and toughness of the biaxially loaded specimens is explained as follows (Fig. 9). Un-

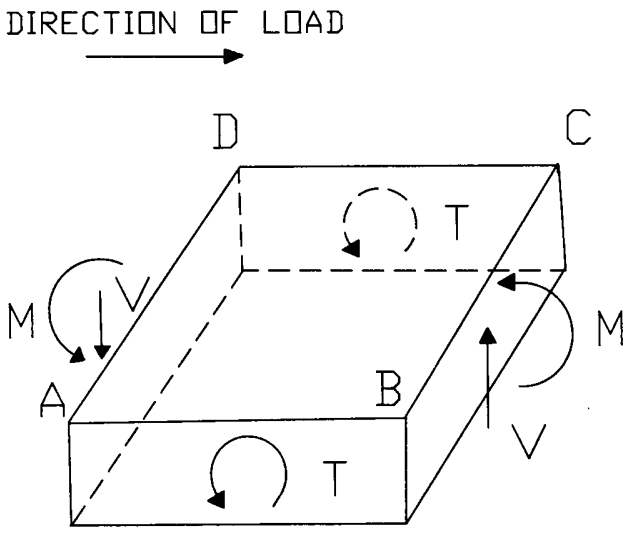

Fig. 9—Forces on connection under uniaxial loading

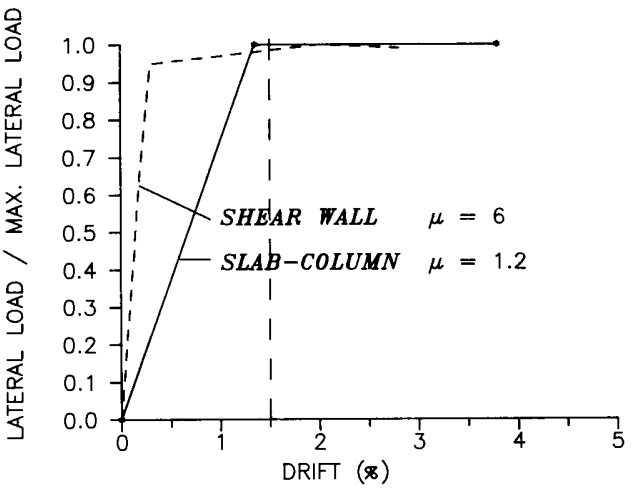

Fig. 10—Comparison of ductility requirements at 1.5 percent drift

der uniaxial loading, resistance is attributable to torsion on Faces AB and CD and shear and moment on Faces BC and DA.[1] If a uniaxially loaded connection is loaded subsequently in the transverse direction, Faces AB and CD (which had previously been loaded in torsion) begin to develop flexure and shear, while Faces BC and DA (which had previously been loaded in moment and shear) begin to develop torsion. The interactions between flexure, shear, and torsion[13] are such that the net connection resistance in any given direction is less under biaxial loading than under uniaxial loading. Similarly, more rapid degradation of the concrete occurs under biaxial loading.

Based on the observations from this series of tests, it is concluded that biaxial lateral loading, as might occur during an earthquake or wind loading, reduces the available strength, stiffness, and overall lateral displacement capacity of slab-column connections. Thus, since most of the data included in Fig. 4 and 5 were obtained from uniaxial tests, conclusions drawn may be on the unconservative side if biaxial loading occurs.

IMPLICATIONS OF THE TEST RESULTS

The data in Fig. 4 and 5 indicate that the available lateral displacement ductility of reinforcement concrete flat-plate connections without shear reinforcement is low by comparison with values often considered marginally acceptable in seismic design.[13] However, the existence of low ductility does not equate de facto with poor performance during a strong earthquake loading. For typical slab-column connections, relatively high flexibility may protect the connections from large displacement ductility demands.

For example, Fig. 10 presents idealized load displacement envelopes of a typical slab-column connection[6] and a slender shearwall[14] that might be used to stiffen a flat-plate building. If the wall is sufficiently stiff to restrain lateral interstory drifts to approximately 1.5 percent of story height (a value occasionally quoted as a reasonable upper bound for severe seismic loading[15]), the required displacement ductility of the wall will be approximately 6. The required displacement ductility of the slab-column connection will be less than 2.

According to the data presented in Fig. 4 and 5, a slab-column connection can be expected to possess some minimal ductility and a drift capacity of at least 1.5 percent of interstory height only if the vertical shear on the connection is less than or equal to approximately 40 percent of the direct punching shear strength. Expressed in terms of shear stresses, the nominal shear stress due to vertical loads should be limited to approximately $(0.4)(4\sqrt{f'_c}) \approx 1.5\sqrt{f'_c}$ psi on the slab critical section. The vertical load should be taken at least equal to the design gravity load shear.

Although it is likely that vertical accelerations during earthquakes (frequently of the same magnitude as the lateral ground accelerations) will further increase the total connection shear, there is no evidence at the present time to prove that this effect should be included when computing the vertical connection shear. Likewise, there is no evidence to confute this possibility.

If gravity loads alone are considered in computing the proposed limiting shear stress, the minimum required column size to satisfy the recommendation is approximately 19 × 19 in. (483 × 483 mm) for a building slab having bays of 20 ft (6.1 m), an 8 in. (203 mm) thick slab, 15 lb/ft² (718 Pa) superimposed dead load, 40 lb/ft² (1915 Pa) service live load, and 4000 psi (27.6 MPa) normal weight concrete. Supporting calculations are in Appendix II.

For lateral interstory drifts exceeding 1.5 percent of interstory height, adequate performance of the flat plate cannot be assured. For this reason, a suitable structural system should be provided to limit lateral drifts.

SUMMARY AND CONCLUSIONS

Experimental data from several investigations are analyzed to identify the parameters that influence the

lateral displacement ductility of reinforced concrete flat-plate connections subjected to lateral loads. Only interior, conventionally reinforced slabs without slab shear reinforcement are considered. Implications of the findings are discussed. The following main conclusions are recapitulated:

1. The magnitude of the gravity load shear carried by the slab is a primary variable affecting the lateral displacement capacity and ductility.

2. For a given level of gravity load, biaxial lateral loading reduces lateral load stiffness, strength, and available ductility.

3. The magnitudes of gravity loads and lateral interstory drifts should be controlled to insure that the integrity of slab-column connections is maintained under seismic loading. Lateral interstory drifts under an extreme earthquake loading should not exceed 1.5 percent of interstory height. At this level of deformation, the available data indicate that the flat-plate connection will perform adequately if the gravity level shear stress acting on the slab critical section does not exceed $1.5\sqrt{f_c'}$.

ACKNOWLEDGMENTS

The authors wish to acknowledge the support of the National Science Foundation and the University of California at Berkeley. The views expressed do not necessarily reflect the views of these organizations.

NOTATION

A_c = area of concrete section resisting shear transfer
b_o = perimeter of critical section for slabs
c_1 = column dimension in the direction of loading
c_2 = column dimension transverse to the direction of loading
D_h = horizontal displacement at the top of column
D_u = ultimate displacement
D_v = difference of the vertical displacement at opposite ends of the slab
D_y = yield displacement
d = distance from extreme compression fiber to centroid of tension reinforcement
d_{avg} = average d
h = overall thickness of slab
h_c = column height
f_c' = compressive strength of concrete
f_y = yield strength of reinforcement
l_1 = length of span in direction of lateral load
l_2 = length of span transverse to l_1
V_g = shear force due to gravity loads
v_{all} = allowable shear stress
V_o = theoretical punching shear strength, Eq. (2)
w_g = dead load
w_l = live load
w_{sdl} = superimposed dead load
w_{slab} = slab self weight
μ = displacement ductility = D_u/D_y

REFERENCES

1. Hawkins, N. M.; Mitchell D.; and Sheu M. S., "Cyclic Behavior of Six Reinforced Concrete Slab-Column Specimens Transferring Moment and Shear," *Progress Report 1973-74,* NSF Project GI-38717, Section II, Department of Civil Engineering, University of Washington, Seattle, 1974, 50 pp.

2. Morrison, Denby G., and Sozen, Mete A., "Response of Reinforced Concrete Plate-Column Connections to Dynamic and Static Horizontal Loads," Civil Engineering Studies, *Structural Research Series* No. 490, University of Illinois, Urbana, Apr., 1981, 560 pp.

3. Ghali, Amin; Elmasri, Mahmoud Z.; and Dilger, Walter, "Punching of Flat Plates Under Static and Dynamic Horizontal Forces," ACI JOURNAL, *Proceedings* V. 73, No. 10, Oct. 1976, pp. 566-572.

4. Islam, Shafiqul, and Park, Robert, "Tests on Slab-Column Connections with Shear and Unbalanced Flexure," *Proceedings,* ASCE, V. 102, ST3, Mar. 1976, pp. 549-568.

5. Hanson, Norman W., and Hanson, John M., "Shear and Moment Transfer Between Concrete Slabs and Columns," *Journal,* PCA Research and Development Laboratories, V. 10, No. 1, Jan. 1968, pp. 2-16.

6. Zee, H. L., and Moehle, J. P., "Behavior of Interior and Exterior Flat Plate Connections Subjected to Inelastic Load Reversals," *Report* No. UCB/EERC-84/07, Earthquake Engineering Research Center, University of California, Berkeley, Aug. 1984, 130 pp.

7. Symonds, D. W.; Mitchell, D.; and Hawkins, N. M., "Slab-Column Connections Subjected to High Intensity Shears and Transferring Reversed Moments," *Progress Report,* NSF Project GI-38717, Department of Civil Engineering, University of Washington, Seattle, Aug. 1976, 80 pp.

8. Newmark, N. M., and Hall, W. J., "Earthquake Spectra and Design," *Engineering Monographs on Earthquake Criteria, Structural Design, and Strong Motion,* Earthquake Engineering Research Institute, El Cerrito, 1982, 103 pp.

9. Kanoh, Y., and Yoshizaki, S., "Experiments on Slab-Column and Slab-Wall Connections of Flat Plate Structures," *Concrete Journal* (Tokyo), V. 13, June 1975, pp.7-19.

10. ACI-ASCE Committee 426, "The Shear Strength of Reinforced Concrete Members—Slabs," *Proceedings,* ASCE, V. 100, ST8, Aug. 1974, pp. 1543-1591.

11. ACI Committee 318, "Building Code Requirements for Reinforced Concrete (ACI 318-83)," American Concrete Institute, Detroit, 1983, 111 pp.

12. Hawkins, Neil M., and Mitchell, Denis, "Progressive Collapse of Flat Plate Structures," ACI JOURNAL, *Proceedings* V. 76, No. 7, July 1979, pp. 775-809.

13. Park, Robert, and Paulay, Thomas, *Reinforced Concrete Structures,* John Wiley & Sons, New York, 1975, 769 pp.

14. Hiraishi, H.; Nakata, S.; and Kaminosono, T., "Static Tests on Shear Walls and Beam-Column Assemblies and Study on Correlation between Shaking Table Tests and Pseudo-Dynamic Tests," *Earthquake Effects on Reinforced Concrete Structures—U.S.-Japan Research,* SP-84, American Concrete Institute, Detroit, 1985, pp. 11-48.

15. Sozen, M.A., "Review of Earthquake Response of Reinforced Concrete Buildings with a View to Drift Control," *State-of-the-Art in Earthquake Engineering,* 7th World Conference on Earthquake Engineering, Istanbul, 1980, pp. 119-174.

16. Moehle, J. P., and Diebold, J., "Experimental Study of the Seismic Response of a Two Story Flat Plate Structure," *Report* No. UCB/EERC-84/08, Earthquake Engineering Research Center, University of California, Berkeley, Aug. 1984, 206 pp.

APPENDIX I—TESTS WITH BIAXIAL LOADING

To investigate the influence of biaxial loading on connection behavior, four tests were conducted by the authors at the University of California at Berkeley. A brief summary of the experimental program follows.

Specimen description

Four identical interior connections were constructed as shown in Fig. A.1. Slab dimensions were 13 × 13 ft (3.96 × 3.96 m) with a thickness of 4.8 in. (121 mm). Column dimensions were 10.8 × 10.8 in. (274 × 274 mm) in cross section, extending 3 ft (0.914 m) above and below the slab. Compressive strength of concrete was specified at 4000 psi (27.6 MPa). Slab reinforcement was all No. 3 Grade 60

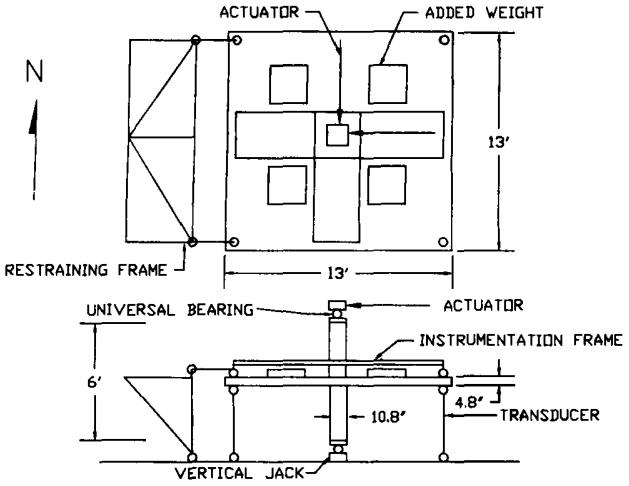

Fig. A.1—Test setup for biaxial loading (1 ft = 0.3048 m; 1 in. = 25.4 mm)

bars (9.53 mm, 414 MPa). The column was heavily reinforced to insure failure at the slab connection region. The slabs were similar in design to those tested previously by Moehle and Diebold[16] and by Zee and Moehle.[6]

Experimental setup

To allow for bidirectional movement, the edges of the slab were supported by steel transducer struts fitted with universal bearings at both ends (Fig. A.1). The top and bottom of the column also were fitted with universal bearings. At the west end of the slab, a torsional restraining frame was attached to reduce in-plane rigid-body twisting of the slab during testing. Two hydraulic load actuators were connected at the top of the column for lateral loading. Gravity load was simulated and maintained at a constant value by adding lead blocks on the slab and by jacking up the bottom of the column. The specimens were instrumented to measure deflections, slab rotations and profiles, reinforcement strains, and secondary displacements.

Test sequence

To investigate the influence of gravity load on connection behavior, high gravity load (0.35 V_o) was imposed on Specimens AP1 and AP2, and low gravity load (0.18 V_o) was imposed on Specimens AP3 and AP4. Specimens AP1 and AP3 were tested with uniaxial lateral loading. Specimens AP2 and AP4 were tested with biaxial lateral loading. Fig. 6 shows the cyclic displacement sequence for the uniaxial tests. The biaxial tests adopted the same sequence but applied in a cloverleaf pattern from Points 1 through 14 of the diagram illustrated in Fig. 6. Plots of lateral force versus drift are shown in Fig. 7 and 8 for the four specimens.

APPENDIX II—SAMPLE CALCULATION OF MINIMUM REQUIRED COLUMN SIZE

Given: h = 8 in. (203 mm); $l_1 = l_2$ = 20 ft (6.1 m); f'_c = 4000 psi (27.6 MPa); w_{adl} = 15 lb/ft² (718 Pa); w_l = 40 lb/ft² (1915 Pa).

Find: Minimum required column size to insure adequate lateral displacement ductility and drift capacity of 1.5 percent.

$d = h - 1.0 = 7$ in.

$w_{slab} = (8/12) \times 150 = 100$ lb/ft²

$w_u = 0.75\,[1.4D + 1.7L + 1.7(1.1E)]$

$= 0.75\,[1.4\,(100 + 15) + 1.7(40)] = 171.75$ lb/ft²

$V_g = 171.75 \times 20 \times 20 = 68{,}700$ lb

$v_{all} = 1.5\sqrt{f'_c} = 94.9$ psi

$A_c = V_g/v_{all} = 68{,}700/94.9 = 723.9$ in.²

$b_o = A_c/d = 723.9/7 = 103.4$ in.

$b_o/4 = 25.9$ in. (assuming square column)

$c_1 = 25.9 - d = 18.9\,(19)$ in. (483 mm)